

Charged-particle multiplicity at mid-rapidity in Au–Au collisions at relativistic heavy-ion collider

D SILVERMYR, for the PHENIX Collaboration
Department of Physics, Lund University, Box 118, 22100 Lund, Sweden

Abstract. The particle density at mid-rapidity is an essential global variable for the characterization of nuclear collisions at ultra-relativistic energies. It provides information about the initial conditions and energy density reached in these collisions. The pseudorapidity densities of charged particles at mid-rapidity in Au+Au collisions at $\sqrt{s_{NN}} = 130$ and 200 GeV at RHIC (relativistic heavy ion collider) have been measured with the PHENIX detector. The measurements were performed using sets of wire-chambers with pad readout in the two central PHENIX tracking arms. Each arm covers one quarter of the azimuth in the pseudorapidity interval $|\eta| < 0.35$. Data is presented and compared with results from proton–proton collisions and nucleus–nucleus collisions at lower energies. Extrapolations to LHC energies are discussed.

Keywords. PHENIX; relativistic heavy-ion collisions; ultra-relativistic heavy-ion collisions; multiplicity.

PACS No. 25.75.Dw

1. Analysis method

The PHENIX experiment is described in detail elsewhere [1]. The main sub-systems utilized in this analysis were the pad chambers (PC) in the central tracking arms, covering 90° in azimuth and $|\eta| < 0.35$, the beam–beam counters (BBC), located in the region $3 < |\eta| < 3.9$ with respect to the center of the detector, and the RHIC-standard zero-degree calorimeters (ZDCs), which detect neutral particles emitted along the beam. Minimum bias triggers were formed using coincidences between the BBC counters and between the ZDC counters. PC, BBC and ZDC provide complementary information on the position of the collision vertex.

The multiplicity analysis uses the layers of pad chambers for vertex and track reconstruction for data obtained with the magnetic field off. The vertex is determined in the following way: The straight lines obtained by combining every hit in PC3 with every hit in PC1 define tracks if they intersect the plane through the beam line within a rectangular window, indicated in figure 1. For each event, the distribution of the intersection points along the z -coordinate (the beam direction) is fitted with a Gaussian function plus a constant. If the fit is successful, the mean of the Gaussian function is accepted as the vertex position of the event. The geometry of PC1 and PC3 and the projection plane is illustrated in figure 1.

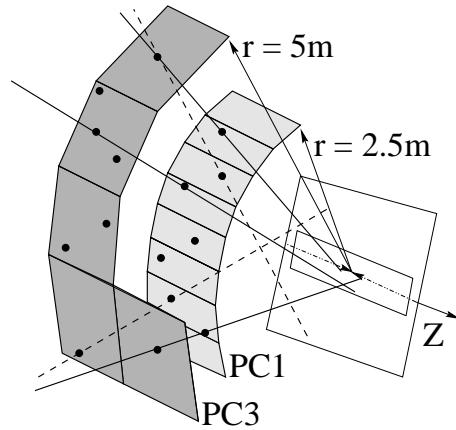


Figure 1. Geometry of the pad chambers. For clarity, three sectors of PC3 are removed from the drawing.

For the track reconstruction, the best available vertex position is used: the first choice is always the vertex derived from PC1/3. For low multiplicity events, where the number of tracks is too small to allow a PC vertex determination, the best choice is the vertex position from the time difference measured by BBC. The agreement between the reconstructed PC and BBC vertices is very good.

Once the vertex position is known, intercepts within a circular window of radius R from the vertex position are accepted. A rather large R cut of 25 cm was used to minimize losses of real tracks. Inherent to the procedure is a combinatorial background contribution, which however can be reliably determined, on the average, by using a technique where each PC1 sector is exchanged with its neighbor. The number of real tracks is then obtained by subtracting the average combinatorial background from the total number of tracks. The analysis method and results from the first run at $\sqrt{s_{NN}} = 130$ GeV are described in detail in ref. [2]. The result for the 5% most central collisions is $dN_{ch}/d\eta = 622 \pm 41$, corresponding to a $dN_{ch}/d\eta$ per participant pair of 3.58 ± 0.26 .

2. Energy dependence of the charged-particle multiplicity

Several measurements of dN_{ch}/dy and $dN_{ch}/d\eta$ at mid-rapidity have been carried out by various experiments at different energies. The results of some of these are compiled in figure 2. The figure incorporates results for the central unit of rapidity from fixed-target heavy-ion experiments at AGS [3], SPS [4], and recent results from RHIC [2,5]. Data from $p-p$ experiments at the ISR, SPS and the Tevatron [6] are also included. The $p-p$ and $A-A$ data show similar trends: approximately logarithmic increase or weak power law dependencies on $\sqrt{s_{NN}}$, although with different coefficients.

To be able to make a relevant comparison of the fixed-target and collider data, the RHIC points need to be scaled to dN_{ch}/dy since $dN_{ch}/d\eta$ is only a good approximation to dN_{ch}/dy at fixed target. At colliders, where the η peak is close to $\eta = 0$, there is a non-negligible suppression of the $dN_{ch}/d\eta$ distribution relative to the dN_{ch}/dy distribution as can be inferred from eq. (1).

Charged-particle multiplicity at mid-rapidity in Au–Au collisions

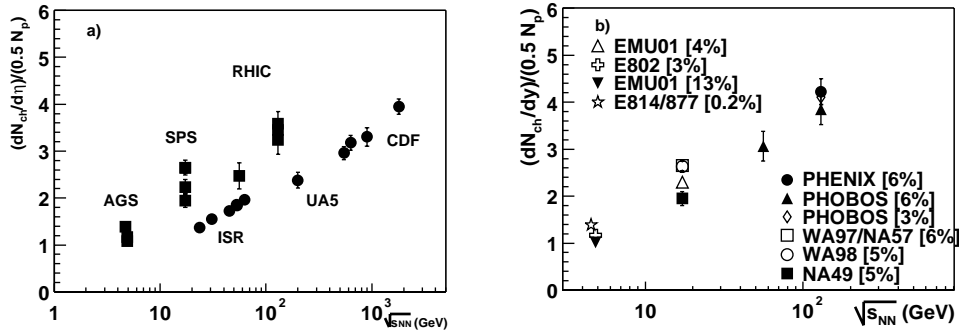


Figure 2. (a) Pseudorapidity density, $dN_{ch}/d\eta$, per participant pair: A – A and p – p data. (b) Rapidity density, dN_{ch}/dy , per participant pair: A – A data.

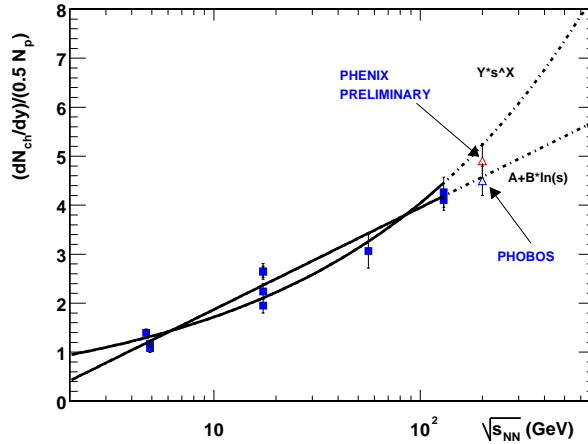


Figure 3. Fits to 10 AA experiments. Published results up to 130 GeV are included in the fits. Note the position of the inserted 200 GeV PHOBOS and preliminary PHENIX points.

$$\frac{d^2 N_{ch}}{dy dp_T} = \frac{d^2 N_{ch}}{d\eta dp_T} \sqrt{1 - \frac{m^2}{m_T^2 \cosh^2 y}}. \quad (1)$$

Since the transverse momentum distributions vary between different models, the obtained scaling factors between $dN_{ch}/d\eta$ and dN_{ch}/dy are somewhat model dependent. According to HIJING, the scaling factors at RHIC at 56 and 130 GeV were roughly 1.2.

An approximately logarithmic scaling of the A – A rapidity density values at mid-rapidity with $\sqrt{s_{NN}}$ is observed in figure 2. To further investigate the nature of the scaling, two different functional forms: $A + B \cdot \ln(s)$, logarithmic increase with s , and $Y \cdot s^X$, power law behavior, previously used to fit p – p data, were fitted to the values of dN_{ch}/dy per participant pair.

The PHOBOS result at 200 GeV [7] of 3.78 ± 0.25 for $dN_{\text{ch}}/d\eta$ per participant pair, is interpreted in ref. [7] as an increase from 130 GeV by a factor of 1.14 ± 0.05 . Preliminary results from PHENIX give an increase in the same quantity by a factor of 1.15 ± 0.04 , while BRAHMS observe a factor of 1.14 ± 0.01 [8].

The fitted functional forms are plotted in figure 3, together with the PHOBOS and preliminary PHENIX 200 GeV points. The points were scaled with the 130 GeV factor to account for the difference between $dN_{\text{ch}}/d\eta$ and dN_{ch}/dy at 200 GeV. This might result in a slightly too high value at 200 GeV, judging from the observed $\sqrt{s_{NN}}$ dependence of the scaling factor. The average at 200 GeV is nevertheless in good agreement with the logarithmic scaling fit. To summarize, the dN_{ch}/dy values for the A–A data studied so far, are well-described by logarithmic scaling with the center-of-mass energy.

Logarithmic scaling predicts an increase of roughly 80% in dN_{ch}/dy per participant pair to LHC, $\sqrt{s_{NN}} = 5500$ GeV, from 130 GeV, while the power law behavior implies an increase of about 300%. The total charged-particle multiplicity will increase with an additional factor due to the widened rapidity region of the produced particles.

From ref. [9], reporting a total charged-particle multiplicity of 4200 at 130 GeV, the equivalent quantity at LHC can be estimated to be about 13,000, assuming logarithmic scaling. If instead the power law fit describes the data, which cannot be excluded by the present analysis due to the uncertainties in the data points at the SPS and RHIC, the total charged-particle multiplicity will be about 30,000 at LHC.

References

- [1] D P Morrison *et al*, PHENIX Collaboration, *Nucl. Phys.* **A638**, 565 (1998)
- [2] K Adcox *et al*, PHENIX Collaboration, *Phys. Rev. Lett.* **86**, 3500 (2001)
- [3] M I Adamovich *et al*, EMU01 Collaboration, *Phys. Lett.* **B322**, 166 (1994)
L Ahle *et al*, E802 Collaboration, *Phys. Rev.* **C59**, 2996 (1999)
J Barrette *et al*, E877 Collaboration, *Phys. Rev.* **C51**, 3309 (1995)
- [4] M I Adamovich *et al*, EMU01 Collaboration, *Phys. Lett.* **B407**, 92 (1997)
M Aggarwal *et al*, WA98 Collaboration, *Euro. Phys. J.* **C18**, 651 (2001)
J Bächler *et al*, NA49 Collaboration, *Nucl. Phys.* **A661**, 45 (1999)
F Antinori *et al*, WA97/NA57 Collaborations, *Euro. Phys. J.* **C18**, 57 (2000)
- [5] B B Back *et al*, PHOBOS Collaboration, *Phys. Rev. Lett.* **85**, 3100 (2000)
- [6] W Thome *et al*, *Nucl. Phys.* **B129**, 365 (1977)
G J Alner *et al*, UA5 Collaboration, *Z. Phys.* **C33**, 1 (1986)
F Abe *et al*, CDF Collaboration, *Phys. Rev.* **D41**, 2330 (1990)
- [7] B B Back *et al*, PHOBOS Collaboration, nucl-ex/0108009
- [8] I G Bearden *et al*, BRAHMS Collaboration, nucl-ex/0112001
- [9] B B Back *et al*, PHOBOS Collaboration, nucl-ex/0106006